# *Commentary on Road Safety*

# Tractrix Trajectory with Slip Steering

Dr Edward Brell BSc MEng PhD and Prof David Thambiratnam BScEng (Hons) MSc PhD
*Queensland University of Technology, Brisbane, Australia*
Corresponding Author: Edward Brell, DrBrell@gmail.com.au, +61 (0) 413 824 447

## Key Findings

The paper considers an urban myth that remedial action for caravan fishtailing is to speed up:

- Using a number of actions that contribute to the fishtailing phenomena the authors highlight the folly of the myth.
- An alternative to the tractrix is presented suggesting scope for adaptation.
- Examples of modified tractrices are presented for two road speeds.
- The results show an earlier cross-over to the next phase of oscillation for the higher speed.
- Angular momentum caused by the tractrix and also windage is greatly affected by vehicle speed.

## Abstract

The tractrix curve, sometimes called the pursuit curve has long been the standard used to describe the path of a pig trailer behind a prime mover. This ideal path still has validity today provided the speed is very low and the trailer is unloaded. During a common phenomenon of snaking or fishtailing, the trailer sways back and forth in relation to the prime mover centreline axis. Often regarded as the nightmare of caravanning, the action does not follow the tractrix curve but follows a shorter path to the common centreline of prime mover and trailer. This paper explores the shorter path in response to a tyre reaction to centripetal force causing slip steer. An example derived by drafting progression steps to show quantitatively that speed causes early cross-over carrying more energy into the next fishtailing phase is presented. It is believed the inclusion of slip steering to modify a tractrix curve is a novel development.

## Keywords

Tractrix, sideslip, pursuit curve, fishtailing, snaking, caravan.

## Introduction

The objective for this paper is to show that when a fishtailing event manifests, where the amplitude of the sway is increasing, speeding up is not a solution to prevent a terminal end. There was scope to choose from a number of causes for the fishtailing and the slip steer modified tractrix posed a particular challenge. Although momentum in the trailer as it rotates from an angle of articulation to zero articulation does not affect slip steering, it is explored to shed more light on the "speeding up" solution.

Highway engineers traditionally used a mechanical device called the Tractrix Integrator or the hatchet planimeter Haynes LC (1931) consisting of a wheel or knife edge at one end of a straightedge and a tracing point at the other end. Historically, famous researchers in the 17th century like Perrault, Newton, Bernoulli, Huygens and Leibnitz amused themselves with a schoolbook tracing a track in the mud, a dog on a leash and a fob watch on a chain. Leibnitz gave the curve the name ***Hundkurve*** translated from German as dog curve. It is believed that Huygens coined the name ***Tractrix***.

Nevertheless, an awkward mathematical expression for the tractrix resulted in the form of ***x = f(y)***, as follows:

$$x = k * \ln(\frac{y}{k-\sqrt{k^2-y^2}})- \sqrt{k^2 - y^2}$$

Where *k* is the length of string. [1]

Attempts have been made to make x the independent variable including a numerical hand-calculator solution by Ross (1987). Sreenavisan et al (2010) present a parametric approach to rotate the axis of hitch point progression by an angle to the x-axis but stop short of integrating the equations needed. Van Aarsen (2018) solved the integration problem and is to be assessed for usefulness in the present context.

It is recognized that the fishtailing phenomenon is complex; involving windage, yaw momentum, centrifugal action and body roll as well as trailer steering of the prime mover. This paper focuses on, and assists in understanding of a limited section of the overall fishtailing cycle.

The objective of this paper is to devise a method to test the trajectory of a trailer on a tractrix path that is modified by slip steering of tyres, in turn influenced by centrifugal action of the trailer mass progressing along a curve. The idea is visualized in Figure 1. In the pursuit of this objective the Van Aarsen (2018) equations are tested to be followed by a tedious manual process of discretizing the trailer path and adding slip steer angles at each step.

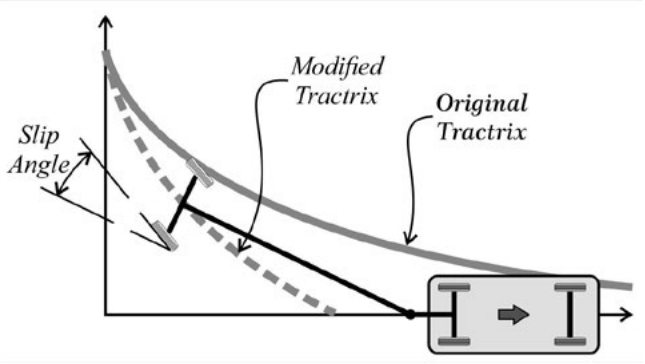


**Figure 1. Idea of side slip progression away from original tractrix**

## Tractrix Curve

Nowadays with modern computers the Equation [1] can be easily plotted. One such plot appears in Figure 2 for a 5.0 m wheelbase trailer.

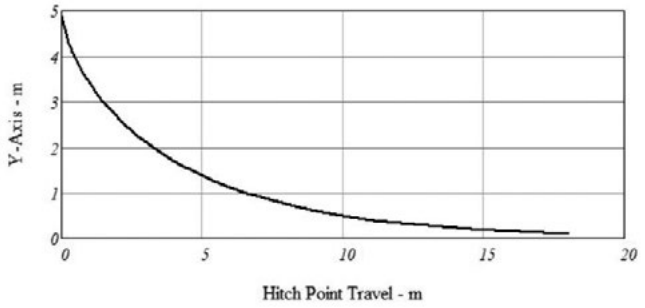


**Figure 2. Graph of slow tractrix curve derived from Equation [1]**

Beyond the use of the tractrix curve is a swept path analysis. Once hand-drawn using a Runge-Kutta style of piecewise stepping method has evolved to modern computer software such as AutoTURN using similar algorithms (Carrasco, 1992).

To show relevance of modern swept paths with the tractrix curve a typical curve is superimposed on a swept path study of right-angled turn of a car and trailer. This is shown in Figure 3.

To offer context for an overall fishtailing cycle, we visualize the trailer's historical path and identify phases. This is shown in Figure 4 where the cycle is divided into 4 phases on the basis of peak oscillation and cross-over across the centreline. This paper considers Phase 4 only.

It should be noted that in the ideal of Phase 4, the wheelbase centreline remains tangent to the tractrix as the tow vehicle

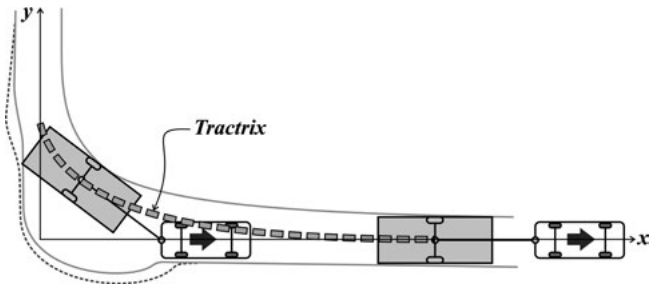


**Figure 3. Tractrix superimposed on a conventional swept path analysis**

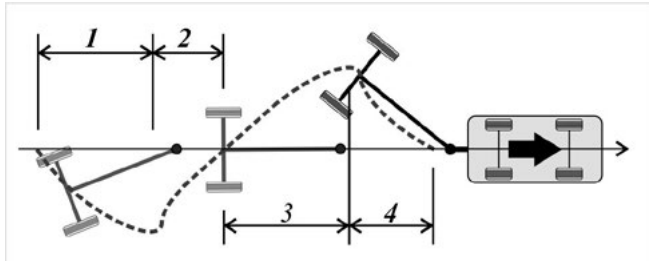


**Figure 4. Historical progression showing phases 1 through 4**

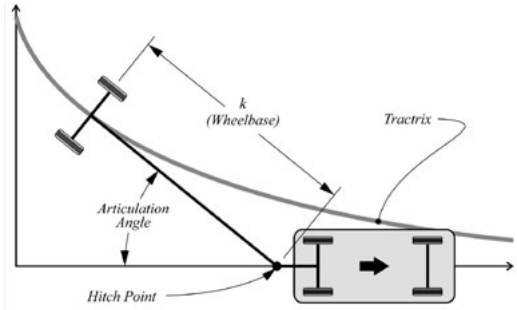


**Figure 5. Trailer skeleton and car superimposed on tractrix curve**

travels on the x-axis, decreasing the articulation angle, asymptotic to the x-axis. It should also be noted that the wheels in the trailer do not slip or twist but have normal forward rolling friction. More description appears in Figure 5.

Slip steering occurs naturally as the tyre contact patch deflects from its original position as a result of the tyre lateral flexibility. It is to be contra-distinguished from a sliding tyre where the traditional Coulomb friction and also adhesive friction factors apply.

Taking the hitchpoint as the frame of reference and given that oscillation is at a standstill at some angular displacement extreme, the trailer begins to revert back to the x-axis. The aberration history is important as an early departure from the original tractrix is cumulative and will affect all future directions of the trailer path. The net effect of slip steering in an oscillation event is that the modified tractrix brings the trailer axle to the x-axis quicker. Nevertheless, in a very slow progression of the hitch point, the axle centre remains asymptotic to the x-axis.

## Alternate Tracking Lines

The modified tractrix idea in Figure 1 on an alternate tracking line held appeal. The authors are indebted to Klaas van Aarsen (2018) for the mathematical gymnastics to produce the following equations:

1. Parallel Tracking Line:

$$x = k * \ln\left(\frac{y-b}{k\sqrt{k^2-(y-b)^2}}\right) - \sqrt{k^2-(y-b)^2} \qquad \textbf{Equation [2]}$$

2. Angled Tracking Line:

$$X(t) = x_c + \frac{k}{\sqrt{(1+m^2)}}[t - \tanh(t) - m(\operatorname{sech}(t) - 1]$$

$$Y(t) = y_c + \frac{k}{\sqrt{(1+m^2)}}[m(t - \tanh(t)) - (\operatorname{sech}(t) - 1]$$

**Equation [3]**

Equations [2] & [3] were developed by Klaas van AArsen (2018) in response to a general enquiry in a mathematics help forum. It was hoped that the equations might find use for trailer articulation.

Equation [2] is merely a tractrix with the hitchpoint following a line parallel to the x-axis. Equation [3] is a tractrix curve with the hitchpoint tracking line at an angle to the x-axis. The visualizations of the new tracking lines appear in Figure 6.

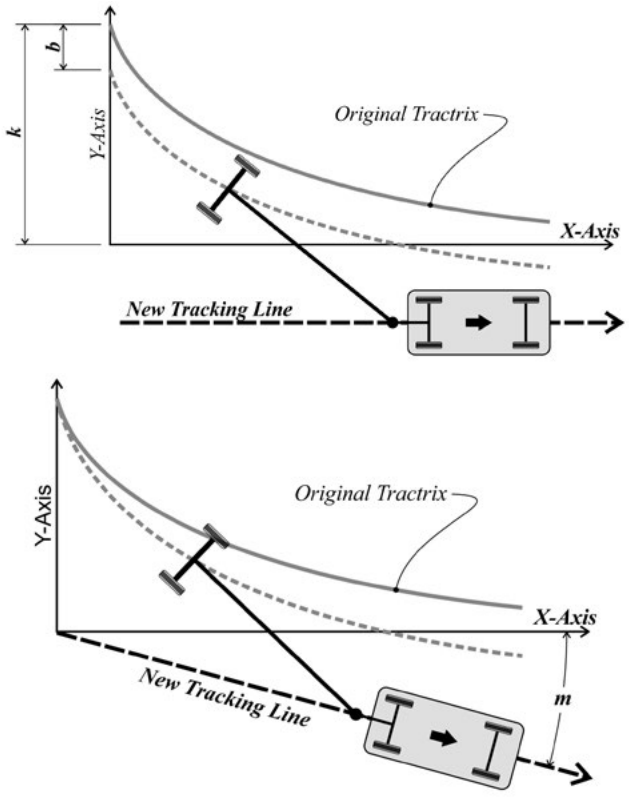


**Figure 6. Visualizations of new tracking lines for modified tractrix**

The input parameters in Equations [2] and [3] are b and m. The two parameters are entered into Equations [2] and [3] left and right respectively in Figure 7 for values b=-0.5 and m=-0.045.

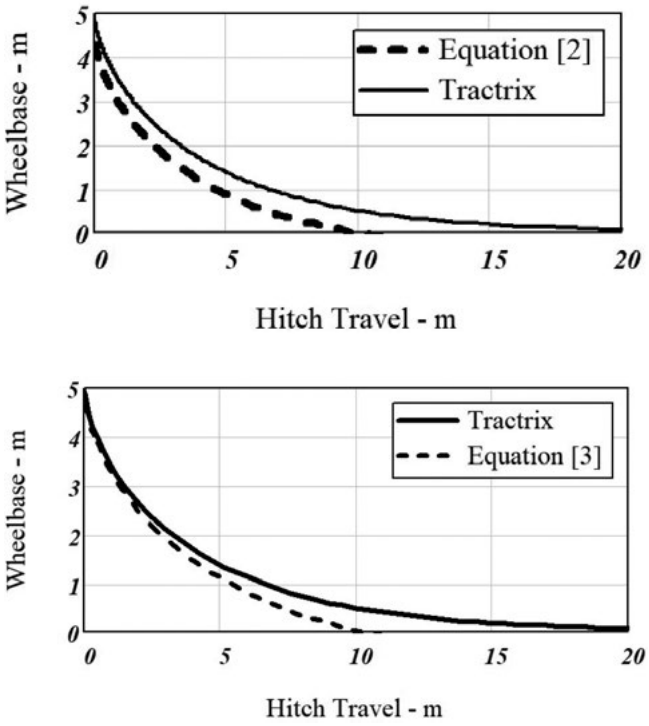


**Figure 7. Plot of modified tractrix for Equations [2] and [3] (left & right respectively)**

Whilst the modified curves cross the x-axis as hoped, the curves were found to be unsuitable for the objectives of this paper as follows:

- There is currently no nexus between the coefficients ***b*** and ***m*** with slip angles
- The curves cannot reflect prime mover speed change.
- Tractrix curvature increases with progression of hitchpoint and so the slip angle must decrease. The slip angles increase in the modified tractrices.
- The curves suggest starting points are at the y-axis. A trailer at right-angles to prime mover cannot have developed sufficient speed to reflect any tyre side slip.

Work is continuing to determine if the curves can be adapted for the present needs.

## Tyre Response

Before we can consider an example of slip steering we must first develop a relationship between lateral tyre force and the angle of slip caused by centrifugal action of the trailer mass following a curved path. For this we use the Pacejka "Magic Formula" (Pacejka, 2012) on a suitable tyre. The well-known formula is shown below:

$$F = F_z * \mathrm{D} * \sin[\,C * \tan^{-1}(B * slip - E * (B * slip - \tan^{-1}(B - slip)))]$$

**Equation [4]**

Here, the coefficients ***B, C, D & E*** describe the particular tyre chosen while ***Fz*** is the vertical force on the tyre. The result is shown below for a trailer weighing 1500 kg (750 kg on each wheel).

A high centre of gravity under centrifugal action will shift load from one tyre to another. A heavier loaded tyre will respond with a greater slip angle and vice versa. To assess whether to ignore the shift in vertical load from the inside wheel to the outside wheel as a result of centrifugal action, values were calculated for a nominal transfer of 100 kg. Curves were calculated and posted to Figure 8.

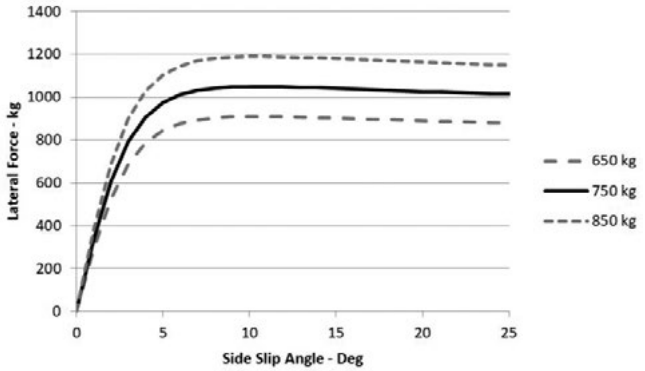


**Figure 8. Lateral forces for side slip angles for varying vertical tyre loads**

The graphs in Figure 8 display typical characteristics of tyre performance under lateral load, as follows:

- The linear portion up to about 3 degrees slip represents pure slip.
- The curved sections are transitional where pure slip combines with sliding.
- The top of the curves represent the maximum limit of tyre adhesion.
- Beyond the top of the curves the tyres are purely sliding with the lateral force developed by adhesive friction declining in magnitude.

In the light of Figure 8, but subject to future study, the 750 kg curve is assumed to be representative of load shifting, as average. A significant simplification follows as a result.

## Graphical Tractrix Modification Example

In the absence of a closed form solution or other suitable mathematical equation that might reflect the effect of slip steering on the path of a vehicle-following trailer, a manual and time-honoured method is employed.

The path of the tow vehicle travels on the x-axis at constant speed. This path is segmented into 0.5 m segments at which calculations are made.

In this analysis, the tow vehicle travels at constant speed. Thus a 90 degree articulation starting point is not practical. The starting point on the tractrix then, is where the oscillation reverses. This nominally occurs at the end of Phase 3 and the start of Phase 4 as shown in Figure 4. Since sideslip history is important, for this example the oscillation is deemed to start at an articulation point having prior developed full centripetal force on the tyres at $10^{O}$.

All parts of the tractrix curvature have an instantaneous radius that increases with progression of the hitchpoint. The resulting centrifugal action can thus be calculated and be shown as centripetal force (Arrow in Figure 9) on the tyre contact patch. Such a force gives rise to slip steering where the wheel direction of heading is different to direction of travel. The science of slip steering is mature and needs little elaboration here. Notwithstanding, slip steering applied to the pursuit curve does not appear to have received adequate coverage. The idea of an instantaneous radius along the tractrix is embodied in Figure 9 (Bronshtein et al, 2007).

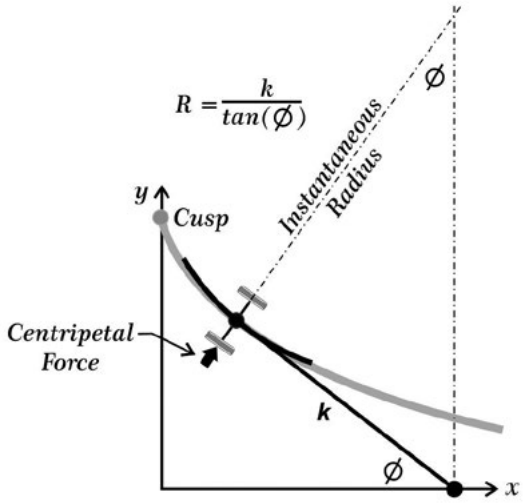


**Figure 9. Calculation of instantaneous radius (R) of tractrix curvature**

It should be noted that as the hitchpoint travels along the x-axis in Figure 9, the instantaneous radius increases. Similarly, the velocity of the trailer wheels increases approaching the constant forward speed of hitchpoint at the lower articulation angles.

A laborious piece-wise construction using accurate drafting software follows, showing reference steps every 0.5 m calculations at which the curvature radius, instant trailer velocity and the corresponding centripetal force are determined for a 5.0 m trailer wheelbase. The reference points showing articulation angles together with lateral forces caused by the ever-changing radii as well as slip angles in degrees are tabulated for two hitchpoint speeds of 60 & 70 km/h.

Beyond the positions #5 and #6 (60 & 70 km/h respectively) the calculations saw little change and created complexity without significant gain. Accordingly, parts of the original tractrix were graphically tacked on as if beyond the points

**Table 1. Tables of lateral force vs. slip angle (degrees) calculated at various trailer positions**

| Hitch Point Speed @ 70 km/h | | | | | Hitch Point Speed @ 60 km/h | | | |
|---|---|---|---|---|---|---|---|---|
| **POSN** | **ARTIC ANG** | **RAD (m)** | **Fc (N)** | **SLIP** | **ARTIC ANG** | **RAD (m)** | **Fc (N)** | **SLIP** |
| 1 | 10.00 | 28.356 | 1020 | 6.30 | 10.00 | 28.356 | 749 | 2.70 |
| 2 | 8.56 | 33.218 | 857 | 4.67 | 8.80 | 32.298 | 640 | 2.15 |
| 3 | 7.29 | 39.085 | 728 | 2.60 | 7.75 | 36.739 | 564 | 1.82 |
| 4 | 6.37 | 44.788 | 635 | 2.13 | 6.85 | 41.622 | 504 | 1.58 |
| 5 | 5.56 | 51.363 | 558 | 1.80 | 6.11 | 46.709 | 447 | 1.38 |
| 6 | 4.86 | 58.805 | 488 | 1.52 | - | - | - | - |

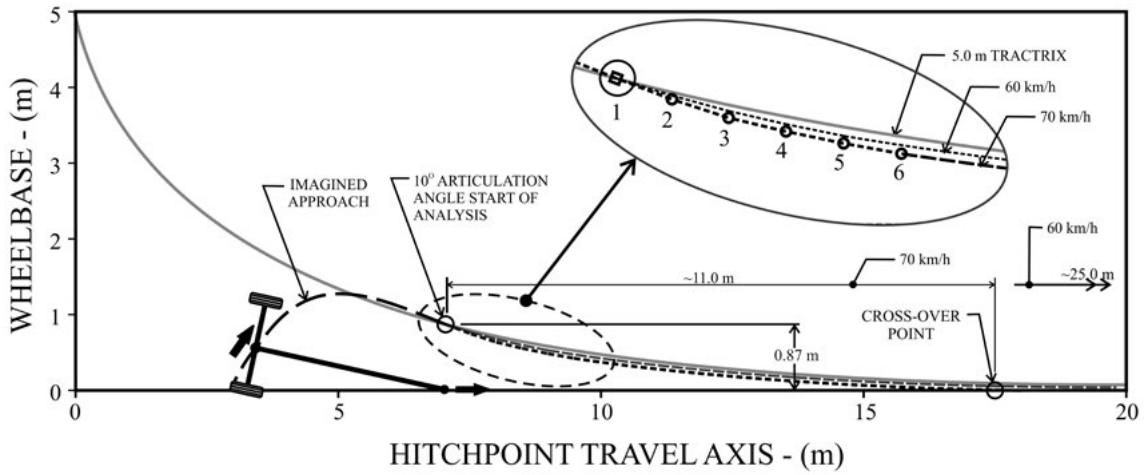


**Figure 10. Technical drafting of variance from true tractrix tracking due to slip angles**

#5 and #6 no more slip steering was occurring. Thus the results shown in Table 1 are conservative, i.e. the real curve aberration from the original tractrix would be larger beyond the points #5 and #6.

From the 10$^{O}$ articulation point to the cross-over point was measured at 11.0 m of hitchpoint travel for the 70 km/h analysis. Not shown for clarity of presentation, the 60 km/h example crossed over at about 25 m.

## Yaw Momentum

As the trailer progresses from the example of 10$^{O}$ articulation angle to the cross-over point, the trailer mass moment of inertia (*I*) gathers momentum. The trailer inertia is acted upon by an inward force at the hitchpoint. The force is impulsive so that acting on the length of wheelbase gives rise to angular momentum, often referred to as yaw momentum.

The trailer mass is assumed to be over the axle and wheelbase intersection. We know from the linear analogue, that:

$$Impulse = Change\ in\ Momentum$$

$$\int Fdt = \Delta(Mv)$$

For the angular equivalent:

$$k \int Fdt = \Delta(I * \omega) \quad \text{where } \omega \text{ is angular velocity}$$

Mass moment of inertia needs to be calculated. An even distribution of mass on a plane area of a caravan in plan view is assumed for a caravan measurement of 5.0 m long x 2.1 m wide. This was calculated at Ames Web, (2018) to be 3676 kgm2. The calculation steps are set out in Table 2 where angular velocity is taken as a linear average.

**Table 2. Calculation of approximate yaw momentum for 60 & 70 km/h analyses**

| Item | For 60 km/h | For 70 km/h |
|---|---|---|
| Hitchpoint Velocity | $Vx = 16.7\frac{m}{s}$ | $Vx = 19.4\frac{m}{s}$ |
| Hitchpoint Distance to Cross-over | $D1 = 25m$ | $D2 = 11m$ |
| Travel Time from $10^O$ to Cross-over | $T1 = \frac{D1}{Vx} = \frac{25}{16.7} = 1.50s$ | $T2 = \frac{D2}{Vx} = \frac{11}{19.4} = 0.57s$ |
| Angular Velocity (Avg.) | $\omega_{avg} = \frac{10°}{T1} = 6.7\ deg/s$ | $\omega_{avg} = \frac{10°}{T2} = 17.7\ deg/s$ |
| Angular Momentum | $L = I * \omega_{avg} = 428\frac{kg*m^2}{s}$ | $L = I * \omega_{avg} = 1134\frac{kg*m^2}{s}$ |

The angular momentum calculated in Table 2 is given as a reasonable approximation using a linearized approach. A more accurate account would involve the curved shape of the angular momentum-time graph. The tractrix between $10^O$ and the appropriate value downstream is reasonably flat and thus a linear approximation simplifies greatly with little loss of accuracy.

To summarize Table 2, for a mere increase of about 17% (from 60 to 70 km/h) in hitchpoint speed, more than twice the cross-over momentum was calculated.

## Windage

Considerations so far have not taken into account the interaction of stagnant air with the speeding caravan. To gain a quantitative appreciation, the authors performed a Computational Fluid Analysis (CFD). Here the vehicles remain stationary while the air has velocity inside a bounding box. Figure 11 shows such a box together with velocity streamers. The 5m long caravan is set at an angle of 10O to the tow vehicle axis.

The model caravan in Figure 11 comprised 33 surfaces exposed to the wind including radiussed corners as well as wheel arches and tyres. The model was set for 60 and 70 km/h wind speed. The spreadsheet output provided forces in the X and Y directions and moment arms about the Z-axis, being the vertically up convention. The forces acting on each surface were resolved into moments about the hitchpoint. The moments about the hitchpoint are reported as follows:

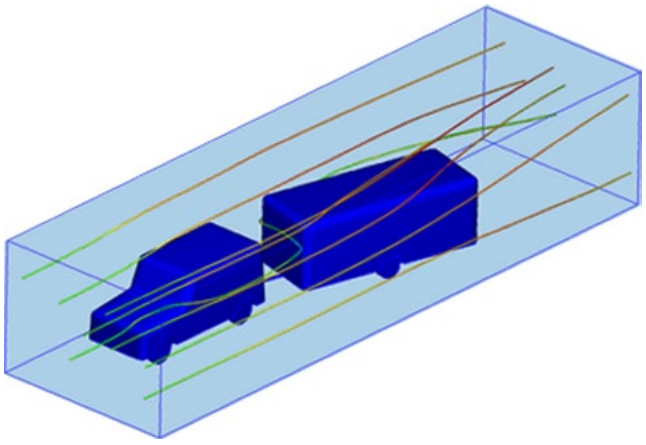

**Figure 11. Car and caravan at 10O articulation in a CFD wind tunnel**

- 60 km/h = 451 kg-m
- 70 km/h = 572 kg-m

These moments acting on a 3.355 m wheelbase offer lateral forces on the tyres at 134 kg and 170 kg for the 60 & 70 km/h respectively. The tyres scoped earlier in this paper for the Pacejka so-called "magic formula" in Figure 8 yielded a modest 0.4 and 0.5 degree slip angle. Whilst modest, they would compound the slip angles calculated to account for the centrifugal actions. Further, laterally softer tyres would provide greater slip angles.

Windage forces causing a moment about the hitch point decrease as the articulation angle decreases. Notwithstanding, these forces acting impulsive over time to zero articulation, add angular momentum to the values listed in Table 2.

To summarise, the computational fluid analysis showed a greater lateral force on the tyres which in turn gave a greater slip angle for the 70 km/h model over the 60 km/h model.

## Conclusion

In this paper we have looked at some factors that contribute to fishtailing of a trailer/caravan in isolation of each other. It is recognised that these factors work in concert with each other to potentially bring about the dreaded out-of-control sway. The paper concludes with the following:

1. Some closed form solutions have been assessed for suitability for current objectives and found to be unsuitable to include slip steering and tow vehicle speed as inputs.

2. A graphical solution has been presented to illustrate that slip steering shortens the time for a towed trailer to cross the hitch straight line path.
3. It was shown in that example that for a mere 17% increase in vehicle speed the cross-over momentum increased to more than twice as compared to the lower vehicle speed..
4. The results of a computational fluid dynamics analysis was presented showing a higher lateral forces on tyres with corresponding higher slip angles of steering for the 70 km/h model as compared to the lower speed.

There is an urban myth that to avoid the terminal consequences of a trailer fishtailing event you need to "drive out of it" by speeding up. The myth has intuitive appeal and hence it remains persistent in the caravanning landscape. It was shown in this paper that a higher vehicle speed gives rise to larger tyre slip and higher cross-over momentum, so fuelling the next oscillation cycle.

The work goes some way in dispelling that myth and suggests that accelerating in a fishtailing event merely makes the terminal end happen at a higher speed.

## Acknowledgements

The substantial help from Juan Carlos Herrera and Klaas van Aarsen in the mathematical areas is gratefully acknowledged. Thanks too, to John Drake of the Drake Trailer Group for the supply of software to power these analyses.

**Funding**: This research did not receive any specific grant from funding agencies in the public, commercial, or not-for-profit sectors.

## References

Ames Web. (2018). *Inertia Calculator*. Retrieved from https://www.amesweb.info/SectionalPropertiesTabs/Mass-Moment-of-Inertia-Rectangle-Plate.aspx: https://www.amesweb.info/SectionalPropertiesTabs/Mass-Moment-of-Inertia-Rectangle-Plate.aspx

Bronshtein, I., & al, e. (2007). *Handbook of Mathematics.* Springer.

Haynes LC, H. F. (1931). THE KNIFE-EDGE OR HATCHET PLANIMETER. *Review of Scientific Instruments*.

Herrera, J. (2018). Tractrix Angular Velocity. *Private Communication*.

Pacejka, H. (2012). *Tire and Vehicle Dynamics.* Delft: Elsevier.

Ross, B. (1987). *The inversion of the tractrix. INT. J. MATH. EDUC. SCI. TECHNOL.*

Sreenavisan, S., & et, a. (2010). A real-time algorithm for simulation of flexible objects. *Mechanism and Machine Theory*.

van Aarsen, K. (2018, November). *Tractrix Line Below the X-Axis*. Retrieved from https://mathhelpboards.com/calculus-10/tractrix-line-below-x-axis-25208-new.html

Weisstein, E. W. (n.d.). *Tractrix*. Retrieved from http://mathworld.wolfram.com/Tractrix.html.